

## The Size of Cryofracture Figures in the Network of Segmented Polyurethane Elastomers

Helena Janik

Technical University of Gdańsk, Faculty of Chemistry, Polymer Technology  
Department, Narutowicza Street 11/12, 80-952 Gdańsk, Poland

**SUMMARY:** Cross-linked segmented polyurethanes were broken below brittle - ductile transition and their fracture surfaces were analysed by optical and electron microscopy. Shapes of polygonal appearance were present on the whole surface of the broken sample, and a radial texture with the fracture origin in the middle of polygons was observed. The average distance between cryofracture and origins ( $L$ ) was measured for each polyurethane studied. The swelling degree was measured and junction-point density calculated. A correlation between  $L$  and the junction-point density,  $\nu$ , has been found to exist.

### Introduction

Studies of the appearance of fracture surfaces (fracture surface morphological features) called the fractography have been used by many researchers to detect possible causes of crack initiation and to understand the fracture process.<sup>1-3)</sup> The studies were done at the macroscale, by visual inspection, and at the microscale by optical and electron microscopy. From the fractographic studies one can identify indirectly the mechanism of polymer failure. The mode of failure mechanism or, in other words, the image observed in the fracture surfaces depends on a variety of factors both of an external (temperature, stress, size and shape of sample, presence of notch, etc.) and an internal nature (molecular weight, crystallinity, entanglements, junction-point density, filler content, impurities, etc.).

The appearance of a fracture surface can be studied at different levels. One can distinguish the macro-<sup>2-5)</sup> (mirror, mist, rough regions) and micro-morphology<sup>2-10)</sup> of the fracture surface (parabolas, ellipses, hyperbolas, mound-depression patterns, river lines, mackerel lines, etc.). In this paper, the micro-morphology of the fracture surface is considered. The micro-fracture morphology has been studied extensively for more than 30 years. Most of the research work has been done on amorphous thermoplastics like polystyrene (PS), poly(methylmethacrylate) (PMMA) or acrylonitrile-butadiene-styrene copolymers,<sup>3,4,11-20)</sup> where craze-dominated brittle fracture occurs. Brittle fracture surfaces in thermoplastics show a variety of structures. For

glassy thermoplastics, the fracture surface morphology has been found to depend not only on the macroscopic parameters such as time, crack speed and stress situation, but also on a microscopic one, namely on the molecular weight. In the case of PMMA, the low molecular weight fraction favours retarded crack growth (RCG), while the high molecular weight one favours normal crack growth (NCG). Thus, the low molecular weight species show RCG and NCG markings, while the high molecular weight materials show NCG and no RCG.<sup>2)</sup>

Thermosetting materials have been studied as well, especially epoxide type polymers. The fracture surfaces of thermosets are often uniformly rough but in some cases oriented level-differences, oriented tear lines or even parabolic markings similar to those obtained in PMMA have been observed. A strong influence of chemical junction points and physical entanglements on the mode of deformation, and hence on the image of fracture surfaces, has been observed in epoxy resins.<sup>21)</sup>

Parabolic markings are examples of the so called coalescence curves<sup>9)</sup> generated by the secondary micro-cracks. The exact shape of coalescence curves in broken samples depends on the ratio of velocities of formation of primary to secondary cracks. Other features, like hyperbolic markings, have been observed predominantly on the fracture surfaces of high molecular weight PMMA. An increasing number of secondary fractures is activated at elevated stress intensity. The observed number of hyperbolic markings on the fractured surface also increases.<sup>2)</sup>

The fractographic analysis of segmented polyurethanes (PUs) has been performed in our laboratory.<sup>22-28)</sup> Careful analysis of micro-fracture morphology of different amorphous PUs that were broken far below the glass transition in the same way, i.e., at constant size and shape of sample and constant temperature, revealed the presence of three types of characteristic markings<sup>23,25,27)</sup> called the radial polygons, pseudo-radial polygons and mound-depression figures. The last were found, so far, only in linear thermoplastics, while the radial polygons were observed in cast network PU.<sup>28)</sup> We have attempted to use fractography to characterise the network structure of the PU. This required the macroscopic parameters of experiments (temperature, shape and size of the sample, etc.) to be constant. We have studied PUs prepared by reaction casting technology. Polymerisation and solidification occurred in the mould simultaneously in a very short time. Since the synthesis of segmented polyurethanes was highly exothermic, many extra reactions could take place depending on the amount of

free reactive isocyanate groups, catalyst level, the temperature inside and outside of the mould, etc. Finally, heterogeneities could develop in the samples.<sup>24,29,30)</sup> All these factors had to be minimized for the fractographic analysis to provide valuable information on the network structure. The breaking should be made well below the brittle-ductile transition of the samples.

In this paper, the results of studies on the junction-point density in relation to the size of polygon-like cryo-fracture figures are presented.

## Experimental Part

All samples were prepared in a two-stage process.<sup>24,31,32)</sup> They were supplied by the laboratories of Technical University of Gdańsk<sup>24)</sup>, Maritime Academy of Gdynia<sup>31)</sup>, and Pittsburgh State University.<sup>32)</sup> The characteristics of the networks segmented polyurethanes are presented in Table 1.

Table 1: Characteristics of segmented polyurethanes.

Sample code	Composition	Non-extractable part /%
CPU-60	PCL/MDI/ BD	98
CPU-1	PPO/MDI/ BD	97.5
CPU-46	AE/MDI/ BD	98
CPU-2	PPO/MDI/BD	99
CPU-12	AE/MDI/BD	98
CPU-07	PPO/MDI/BD+TMP	99
CPU-27	PPO/MDI/BD	99
CPU-08	PPO/MDI/TMP	98
CPU-7	AEB/MDI/EAG+CP	96
CPU-508	PPO/MDI/TMP	96

PPO: poly(oxypropylene) diol, AE: poly(ethylene adipate) diol, AEB: poly(ethylene/butylene adipate) diol, PCL: poly(caprolactone) diol, MDI: 4,4'-diphenylmethane diisocyanate, BD: butanediol, TMP: trimethylolpropane, AEG:  $\alpha$ -allyl glycerine ether, CP: dicumyl peroxide. All diols had average molecular weights ca. 2000.

The samples with symbols CPU-60, CPU-1, CPU-46, CPU-2, CPU-12, CPU-27 were formed with networks by allophanate bonds<sup>33,34)</sup>, while in the samples CPU-07, CPU-08, CPU-508 the branching agent was trimethylolpropane (TMP), a trifunctional chain extender. All

samples were amorphous. Those obtained from the same components, but at a different temperature or catalyst level, have different codes in Table 1 (e.g., CPU-1 vs. CPU-2 or CPU-27). More information about the sample preparation can be found elsewhere.<sup>24,31,32)</sup>

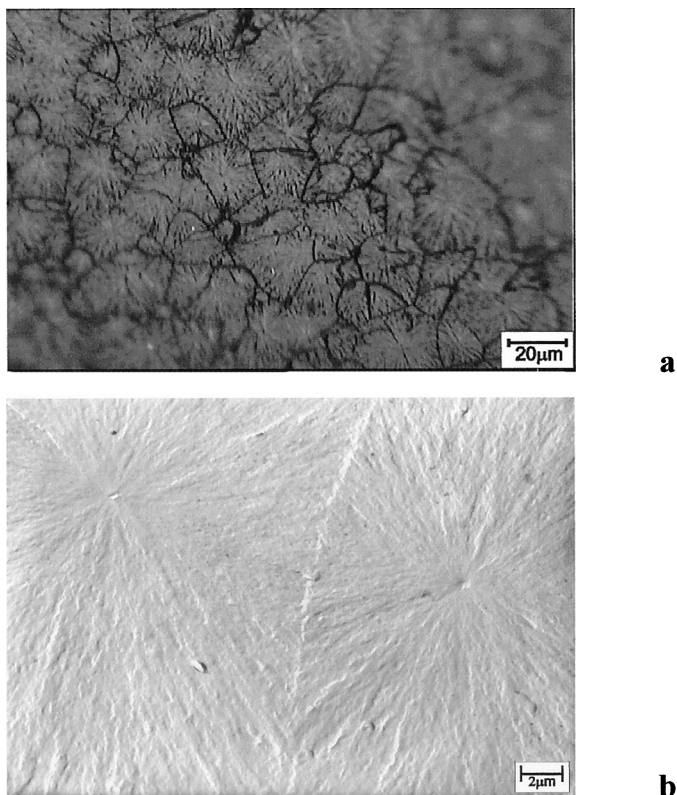


Fig. 1: Examples of the micro-morphology of cryo-fracture surface in a PU broken below brittle-ductile transition (sample CPU-60); **a**. metallographic microscope, **b**. electron microscope. The radial texture and micro-fracture origins are visible in all the PU samples.

Specimens of size 2×2×30 mm were cut out from the bulk material, put into clamps, and manually broken after keeping them for 5 min in liquid nitrogen. The fracture surfaces of the specimens were observed in a transmission electron microscope (TEM) and a metallographic microscope (MM) equipped with a TV camera connected to a computer. Two-step replicas were used for TEM.<sup>24)</sup>

Similar specimens were placed in tetrahydrofurane (THF) at 25°C until swelling equilibrium was reached (in approximately 3 days). The degree of swelling  $q$  was calculated from the

weight ratio of swollen to dry sample. In order to evaluate the junction-point density using the equilibrium swelling method,<sup>35)</sup> additional measurements were made at 35, 45, and 55°C.

Results and Discussion

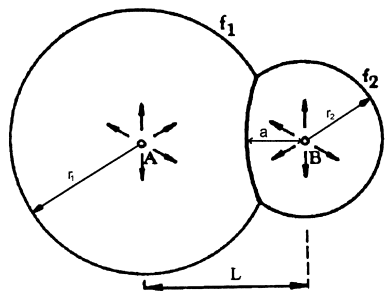


Fig. 2: The scheme of coalescence figures representing images seen in Fig. 1 (detailed description in the text).

Polygons and sometimes hyperbolas with a radial texture and micro-fracture origins inside were found over the whole broken surfaces of all the polyurethanes studied (Fig. 1). The size of figures was different in different samples. The distance,  $L$ , between the micro-fracture origins (points A and B in Fig. 2), from which spread the primary ( $f_1$ ) and secondary ( $f_2$ ) micro-fracture fronts<sup>26)</sup>, was chosen as a parameter describing qualitatively the fracture surface figures (Fig. 2).

Table 2: The distance between micro-fracture origins,  $L$ , swelling degree,  $q$ , and junction-point density,  $\nu$ , for the PU samples.

Sample code	$L$ / $\mu\text{m}$	$q$	$10^4 \cdot \nu$ / $\text{mol} \cdot \text{cm}^{-3}$
CPU-60	17.6	4.76	0.17
CPU-1	24.8	3.88	1.02
CPU-46	26.2	3.05	6.26
CPU-2	36.9	3.03	7.12
CPU-12	37.5	2.90	7.10
CPU-07	38.4	3.10	7.12
CPU-27	39.5	2.79	11.23
CPU-08	40.4	2.72	12.05
CPU-7	41.2	2.33	13.72
CPU-508	56.7	1.78	20.64

The results of swelling experiments and the junction-point densities calculated therefrom are also shown in Table 2. The additional check on the character of the time dependence of swelling degree and on the correlation between swelling degree and the junction-point densities expressed in terms of the number of moles of networks chains per unit volume,  $\nu$ , showed no unexpected behaviour during the swelling experiments.

Fig. 3 shows the linear correlation between  $\nu$  and  $L$ , that represents the characteristics of cryo-fracture surface. Thus, the analysis of the cryo-fracture surface can serve as a new quantitative method of PU network characterisation.

The test is very quick and takes about 10 min. as compared to 3 days procedure needed to perform swelling tests and calculate junction-point density. The cryo-fracture analysis can be accomplished in a laboratory or in an industrial plant for examining the quality (reproducibility) of PU elements by analysing a very small sample under metallographic or electron microscopes. The sample should not have any macro defects.

Further experiments are in progress to confirm the results for more samples. Supposedly, in the future the correlation between junction-point density and the parameter  $L$  will be used as a kind of calibration curve (evaluated separately for particular systems) for quickly estimating the junction-point densities or at least the state of the defects in the PU sample from the cryo-fracture test.

The question arises concerning the nature of different amounts of micro-fracture origins when the junction-point density is changed. One of the explanations found in the literature is that the network forming process introduces micro-heterogeneities into the network that might affect macroscopic behaviour of the polymer.<sup>36)</sup> The free ends can represent some kind of micro-heterogeneity as each free end causes an "empty place" acting as a source of stress concentration.<sup>4)</sup> One can imagine a situation when an increase of junction points reduces the number of defects<sup>37)</sup> on the molecular level, for example, dangling chains. However, these remarks are merely speculations and further research by neutron scattering or solid state NMR could extend our understanding the relations found experimentally.

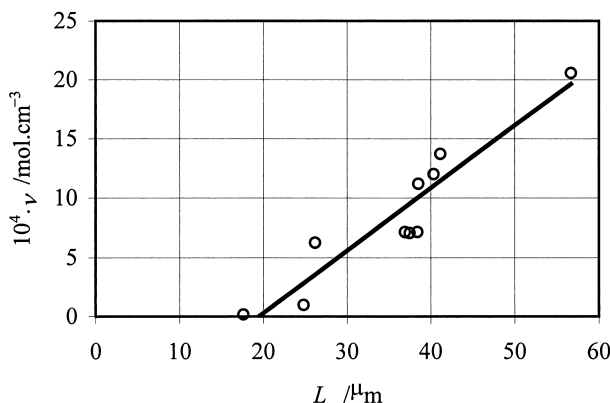


Fig. 3: The junction-point density,  $\nu$ , as a function of  $L$  for the PUs studied.

## Conclusion

The relationship between the average distance of the micro-fracture origins,  $L$ , (characterising the size of cryo-fracture figures) and junction-point density,  $\nu$ , has been found for network PUs obtained using a two stage process. The results are proposed as the basis of a method of characterising the quality of network polyurethanes by the microscopic observation of cryogenically broken samples.

## References

1. H. H. Kaush, "Polymer Fracture", Springer, Berlin, 1988, p. 200
2. A. C. Roulin-Moloney, "Fractography and Failure Mechanisms of Polymers and Composites", Elsevier, London, 1989, chap. 7-11
3. R. J. Bird, J. Rooney, G. Mann, *J. Polymer* **12**, 742 (1971)
4. I. Wolock, S. B. Newman, in: "Fracture Processes in Polymeric Solids", B. Rosen (ed.), Interscience, New York 1964, chap. 2C
5. A. Siegman, A. Hiltner, *Polym. Eng. Sci.* **24**, 869 (1984)
6. F. Lednický, *Polym. Bull. (Berlin)* **11**, 579 (1984)
7. M. J. Doyle, *J. Mat. Sci. Lett.* **10**, 159 (1975)
8. M. J. Owen, R. G. Rose, *J. Mat. Sci.* **10**, 1711 (1975)
9. F. Lednický, Z. Pelzbauer, *J. Polym. Sci. Part C*, **38**, 375 (1972)
10. R. P. Kusy, D. T. Turner, *Polymer* **18**, 391 (1977)
11. P. Beahan, M. Bevis, D. Hull, *J. Mat. Sci.* **8**, 162 (1973)
12. D. L. Lainchbury, M. Bevis, *J. Mat. Sci.* **11**, 2222 (1976)

13. D. L. Lainchbury, M. Bevis, *J. Mat. Sci.* **11**, 2235 (1976)
14. J. A. Sauer, C. C. Chen, *Polym. Eng. Sci.* **24**, 786 (1984)
15. D. Kells, N. J. Mills, *J. Mat. Sci.* **17**, 1963 (1982)
16. M. Doyle, *J. Mat. Sci.* **8**, 118 (1973)
17. W. Doll, *Adv. Polym. Sci.* **53**, 106 (1983)
18. J. Hoare, D. Hull, *J. Mat. Sci.* **10**, 1861 (1975)
19. M. Parvin, J. G. Williams, *J. Mat. Sci.* **10**, 1883 (1975)
20. C. C. Chen, J. A. Sauer, *J Appl. Polym. Sci.* **40**, 503 (1990)
21. M.Glad, "*Microdeformation and network structure in epoxides*", PhD Thesis, Cornell University, Ithaca, 1986
22. J. Foks, H. Janik, S. Winiecki, *J. Appl. Polym. Sci.* **27**, 645 (1982)
23. J. Foks, H. Janik, in "*Morphology of Polymers*", B. Sedláček (ed.), Walter de Gruyter C., Berlin 1986, p. 559
24. J. Foks, H. Janik, *Polym. Eng. Sci.* **29**, 113 (1989)
25. H. Janik, "*Morphology and some properties of cast polyesterurethanes*," PhD. Thesis, Technical University of Gdańsk, Poland, 1989
26. J. Foks, G. Michler, *J. Appl Polym. Sci.* **31**, 1281 (1986)
27. H. Janik, J. Foks, *Progr. Colloid Polym. Sci.* **90**, 241 (1992)
28. H. Janik, *J. Macromol. Sci.-Phys.* **B38**, 981 (1999)
29. J. D. Fridman, E. L. Thomas, L. J. Lee, C. Macosko, *Polymer* **21**, 393 (1980)
30. R. M. Briber, E. L. Thomas, *Polymer* **25**, 171 (1984)
31. M. Rutkowska, A. Kwiatkowski, *J. Polym. Sci.* **53**, 141 (1975)
32. Z. Petrovic, I. Javni I, V. Divjakovic, *J. Polym. Sci. Part B.* **36**, 221 (1998)
33. J. H. Saunders, *Rubber Chem. Technol.* **33**, 1259 (1960)
34. K. Gilding, S. A. Dixon, <http://www.biomaterials-partnership.org.uk>
35. B. E. Conway, S. C. Tong *J. Polym. Sci.* **46**, 113 (1960)
36. T. Vilgis, *Progr. Colloid Polym. Sci.* **90**, 1 (1992)
37. E. J. Kramer, Cornell University, private communication 1996